nature publishing group

Pulmonary *M. tuberculosis* infection delays Th1 immunity via immunoadaptor DAP12-regulated IRAK-M and IL-10 expression in antigen-presenting cells

M Jeyanathan[1,2,3], S McCormick[1,2,3], R Lai[1,2], S Afkhami[1,2], CR Shaler[1,2], CN Horvath[1,2], D Damjanovic[1,2], A Zganiacz[1,2], N Barra[1,2], A Ashkar[1,2], M Jordana[1], N Aoki[1] and Z Xing[1,2]

Interaction of mycobacteria with the host leads to retarded expression of T helper cell type 1 (Th1) immunity in the lung. However, the immune mechanisms remain poorly understood. Using *in vivo* and *in vitro* models of *Mycobacterium tuberculosis* (*M. tb*) infection, we find the immunoadaptor DAP12 (DNAX-activating protein of 12 kDa) in antigen-presenting cells (APCs) to be critically involved in this process. Upon infection of APCs, DAP12 is required for IRAK-M (interleukin-1 receptor-associated kinase M) expression, which in turn induces interleukin-10 (IL-10) and an immune-suppressed phenotype of APCs, thus leading to suppressed Th1 cell activation. Lack of DAP12 reduces APC IL-10 production and increases their Th1 cell-activating capability, resulting in expedited Th1 responses and enhanced protection. On the other hand, adoptively transferred DAP12-competent APCs suppress Th1 cell activation within DAP12-deficient hosts, and blockade of IL-10 aborts the ability of DAP12-competent APCs to suppress Th1 activation. Our study identifies the DAP12/IRAK-M/IL-10 to be a novel molecular pathway in APCs exploited by mycobacterial pathogens, allowing infection a foothold in the lung.

INTRODUCTION

Pulmonary tuberculosis (TB) caused by *Mycobacterium tuberculosis* (*M. tb*) has haunted humans for many centuries. TB currently accounts for ~1.4 million deaths, secondary only to HIV/AIDS, and 9 million new cases each year.[1] The continuing global TB epidemic emphasizes the importance of improving our limited knowledge in host defense mechanisms to developing effective preventive and therapeutic strategies.[2,3]

Robust T cell-mediated T helper type 1 (Th1) immunity is essential to effectively control *M. tb* replication within the primary target antigen-presenting cells (APCs), the alveolar macrophages,[4] and dendritic cells (DCs).[5] It is widely believed that one of the most important roles of Th1 cells in anti-TB host defense is to produce interferon-γ (IFN-γ) required for activation of infected APCs to control bacterial replication.[6] However, relative to many other types of respiratory intracellular infections, pulmonary mycobacterial infection via its robust immune-suppressive property significantly delays the induction of Th1 responses in the lung. Indeed, a significant number of anti-TB Th1 cells do not begin to enter the lung until 18–20 days after *M. tb* exposure, resulting in much delayed lung protection.[7–11] Such delayed expression of protective Th1 immunity in the lung has been linked to delayed T-cell priming in the draining lymph nodes (dLNs).[10] It has been found that even parenteral immunization accelerates the expression of Th1 immunity in the lung only by ~3–4 days.[11,12] Thus, delayed Th1 immunity allows *M. tb* a significant period of time to go unchecked and establish a strong foothold in the lung.[12–15] However, in spite of some recent progress,[16–19] the cellular and molecular immune mechanisms hijacked by mycobacterial infection to retard Th1 immunity still remain poorly understood. This has recently been identified as an issue of paramount importance in the fight against TB.[12,14,15]

[1]McMaster Immunology Research Centre and Department of Pathology and Molecular Medicine, Hamilton, Ontario, Canada and [2]Michael G. DeGroote Institute for Infectious Disease Research, McMaster University, Hamilton, Ontario, Canada. Correspondence: Z Xing (xingz@mcmaster.ca)
[3]The first two authors contributed equally to this work.

Received 6 May 2013; revised 4 September 2013; accepted 23 September 2013; published online 30 October 2013. doi:10.1038/mi.2013.86

The initial infection of APCs by mycobacteria in the lung represents the first point of host–microbe interaction that leads to a series of host responses. The initiation of Th1 cell activation requires the effective communication of functionally activated APCs with naive T cells via antigen (Ag) presentation and other cognate interactions in the dLNs. One of the APC surface molecules that regulate APC activation is a transmembrane signaling immunoadaptor molecule named DAP12 (DNAX-activating protein of 12 kDa), expressed primarily by APCs such as DCs and macrophages.[20–23] Mounting evidence from us and others indicates that DAP12 has a dual role, activating or inhibitory, in inflammatory and immune responses, depending on the target immune cell type, the nature of infectious agents, and variation in animal models, as well as on which of its associated nonsignaling receptors, including MDL-1, TREM-1 (triggering receptor expressed on myeloid cells 1), and TREM-2, DAP12 pairs with.[24–32] Expression of DAP12 and some of its associated receptors was previously found to be upregulated on pulmonary mycobacterial infection.[33] Recent emerging evidence has suggested an immune regulatory role by DAP12 pathway in Th1 cell activation during pulmonary mycobacterial infection by *Mycobacterium bovis* Bacillus Calmette–Guérin (BCG).[29] However, whether DAP12 plays a critical regulatory role in Th1 responses to pulmonary *M. tb* infection is still unclear, and both the cellular and molecular mechanisms of DAP12-mediated Th1 immune regulation have remained poorly understood.

In our current study we have used a number of *in vivo* and *in vitro* approaches to investigate the role of DAP12 in the regulation of Th1 immune activation during pulmonary *M. tb* infection. We have revealed that the DAP12 signaling pathway in APCs represents an important mechanism involved in mycobacterium-mediated delay in the expression of Th1 immunity in the lung. We have further identified that DAP12 restricts Th1 cell activation via its regulatory effects on interleukin-1 receptor-associated kinase M (IRAK-M) and interleukin-10 (IL-10) expression in pulmonary APCs.

RESULTS

Lack of DAP12 pathway leads to enhanced immune protection against pulmonary mycobacterial infection

We have previously shown that DAP12 expression was induced both at mRNA and protein production levels after pulmonary mycobacterial infection.[33] To examine the role of DAP12 in host defense against pulmonary tuberculous infection, wild-type (WT) and DAP12-deficient (DAP12 knockout (KO)) mice were challenged via the respiratory tract with *M.tb*H37Rv and bacterial burden in the lung and spleen were assessed at 2 and 4 weeks after infection. At 2 weeks, both WT and DAP12 KO animals had comparable levels of bacterial burden in the lung and the spleen (**Figure 1a**). However, at 4 weeks after infection, DAP12 KO animals had much lower levels of bacterial burden (>1 log reduction) in the lung than WT animals (**Figure 1b**). Similarly, when challenged with *M.tb*H37Ra, although both WT and DAP12 KO animals had similar bacterial burdens in the lungs at 2 weeks, DAP12 KO animals had $\sim$1 log fewer bacilli in the lungs than WT animals at 4 weeks after infection (data not shown). The levels of bacterial burden in the spleens of DAP12 KO animals were also lower between 2 and 4 weeks after infection compared with those in WT controls (**Figure 1a,b**).

To examine the potential tissue inflammatory–immune basis for the differential protective levels seen in WT and DAP12 KO hosts, we compared histopathological changes in the lungs harvested from 2- and 4 week-challenged animals. We found that although WT mouse lungs displayed minimal inflammation at 2 weeks, DAP12 KO lung tissues had overt inflammatory infiltrates in the peripheral bronchial and vascular areas (**Figure 1c**). By 4 weeks after infection, there were discrete granulomatous foci formed in the lung of WT animals (**Figure 1d**). In comparison, the granulomatous responses were much more

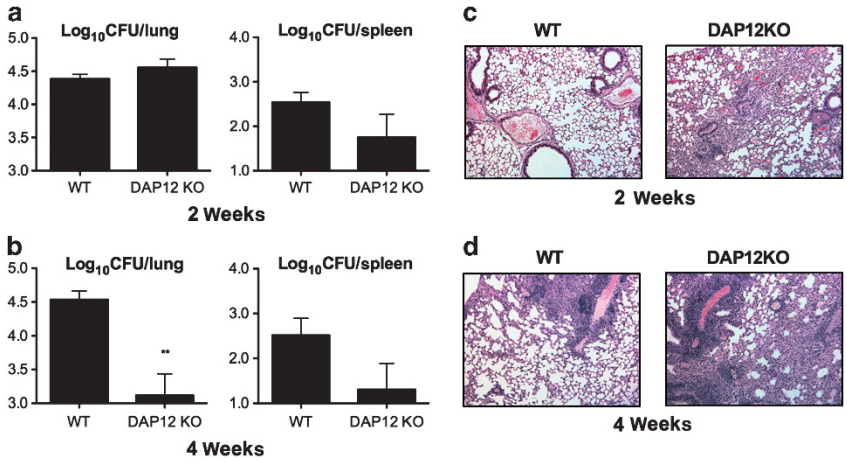

Figure 1 Lack of DAP12 (DNAX-activating protein of 12 kDa) enhances immune protection against pulmonary mycobacterial infection. Groups of wild-type (WT) and DAP12 knockout (KO) mice were killed (**a**, **c**) 2 weeks or (**b**, **d**) 4 weeks after *M.tb*H37Rv challenge. (**a**, **b**) Mycobacterial counts in the lungs and spleens were evaluated using colony-forming assay. Results are expressed as mean ± s.e.m. of colony-forming units (CFUs) from five to six mice per group, representative of two independent experiments. Representative light micrographs depict $\times$10 magnification of hematoxylin and eosin-stained lungs of WT and DAP12 KO mice at (**c**) 2 weeks or (**d**) 4 weeks after mycobacterial infection. $^{**}P<0.01$.

intensified and there was also diffused inflammatory infiltration in the alveolar areas in the lung of DAP KO animals (**Figure 1d**). These data together suggest that lack of DAP12 signaling pathway results in enhanced immune protection from pulmonary *M. tb* infection, which is associated with enhanced tissue granulomatous responses.

Mycobacterial infection leads to delayed Th1 cell responses in the lung via DAP12 pathway

As the timing of the arrival of Th1 cells at the lung correlates with the rising levels of lung immune protection,[7,13,34,35] and we have observed intense tissue inflammatory responses in the lung of DAP12 KO animals in the early course of infection (**Figure 1c,d**), we set out to examine the early kinetics of Th1 immune responses in the lung of WT and DAP12 KO mice following *M. tb* infection. Given similarly enhanced protection seen in the lung of H37Ra-infected DAP12 KO animals described above and the technical constraint in using the virulent strain for detailed mechanistic investigations, we used *M.tb*H37Ra for detailed immunologic analysis. We found that the number of total CD4 T cells into the lung was markedly greater in DAP12 KO mice at day 5 (d5), d7, or d14 after infection (data not shown). Accompanied with enhanced total T-cell infiltration was quicker emergence and enhanced responses of IFN-γ-secreting Ag-specific Th1 T cells in the lung of DAP12 KO mice compared with their WT counterparts (**Figure 2a–c**). In particular, Ag-specific Th1 cells were not detectable at d5 and did not significantly increase until d14 after infection in the lungs of WT mice (**Figure 2a–c**). On the contrary, such cells were readily detectable in the lungs of DAP12 KO mice as early as d5 (2.1% vs. 0.1% in WT) (**Figure 2a**) and they were significantly 2–3 times greater than WT controls at the time points examined (d5, d7, and d14) after infection (**Figure 2a–c**).

To further verify the role of DAP12 in regulating Th1 immune responses in the lung, we reconstituted DAP12 in the lungs of DAP12 KO mice before infection by using a viral-based gene transfer vector expressing transmembrane DAP12 (AdDAP12)[31] (**Figure 2d**). As a control, a set of DAP12 KO mice received only the empty control vector (Addl). The level of Ag-specific Th1 cell responses in the lung was examined at d14 after infection. Compared with the control mice, indeed DAP12 reconstitution in DAP12 KO animals significantly reduced the levels of Th1 cell responses in the lung (Addl $4.0 \pm 0.24\%$ vs. AdDAP12 $2.4 \pm 0.2\%$; $P \leq 0.01$; **Figure 2e**). The above data together suggest that pulmonary mycobacterial infection leads to delayed Th1 cell responses in the lung and that DAP12 pathway represents an important mechanism that mediates delayed Th1 responses. Thus, the disruption of DAP12 pathway results in accelerated expression of Th1 immunity and subsequently enhanced protection in the lung.

Mycobacterial infection suppresses proinflammatory but increases anti-inflammatory cytokine responses in the lung via DAP12 pathway

To begin to understand the mechanisms by which DAP12 pathway suppresses Th1 immunity to *M. tb* infection in the lung, we assessed the levels of both proinflammatory and anti-inflammatory cytokines in the lungs of infected WT and DAP12 KO animals at d7, d14, and d21. In line with the intracellular cytokine staining data (**Figure 2**), there were remarkably higher levels of Th1 cytokine IFN-γ protein in the lungs of infected DAP12 KO mice compared with WT controls at all time points (**Supplementary Figure S1A** online). In comparison, the levels of IL-12 were comparable in the lungs of both WT and DAP12 KO animals at d7 and d14, but at d21 significantly higher levels of IL-12 were seen in the lungs of DAP12 KO mice (**Supplementary Figure S1B**). We also measured the levels of a prototypic proinflammatory cytokine tumor necrosis factor-α (TNF-α) known to be critical to anti-TB Th1 immunity.[6,36] We found that the levels of TNF-α protein in the lungs of infected DAP12 KO mice were much significantly higher at d7, d14, and d21 than in WT counterparts (**Figure 2f**). We further determined the major cellular sources of contribution to differential TNF-α production in the lung by performing intracellular cytokine staining with lung mononuclear cell samples collected at d14 after infection. We found much greater numbers of TNF-α+ APCs as compared with TNF-α+ CD4 T cells in the lungs of both infected WT and DAP12 KO mice. However, DAP12 KO lungs had almost twice as many TNF-α+ APCs as WT counterparts (**Supplementary Figure S2**). They also had significantly more TNF-α+ CD4 T cells than WT controls (**Supplementary Figure S2**). These data suggest the DAP12 KO APCs to be the main contributor to heightened TNF-α production in the lung.

Much heightened proinflammatory cytokine responses to mycobacterial infection resulting from DAP12 disruption prompted us to assess the levels of immune-suppressive cytokine IL-10 in the lung. It is known that once in the lung, mycobacterial pathogens exploit some of the well-known host's immune-regulatory mechanisms such as IL-10 to counter Th1 immune activation for their survival and replication benefits.[37–40] Indeed, opposite to much heightened TNF-α (**Figure 2f**) and IFN-γ (**Supplementary Figure S1A**) responses, the lungs of infected DAP12 KO animals had significantly reduced levels of IL-10 than in WT controls, particularly at d14 and d21 after infection (**Figure 2g**). Thus, these data together suggest that DAP12 plays a role in decreased pro-inflammatory/Th1 and increased immune-suppressive cytokine responses in the lung following mycobacterial infection.

Mycobacterial infection suppresses the activation of APCs in the lung via DAP12 pathway

To further investigate the mechanisms by which DAP12 pathway suppresses proinflammatory cytokine responses and Th1 immunity to *M. tb* infection in the lung, we examined the activation status and functionality of the APCs in the lung, as APCs including DCs and macrophages play an essential role in early innate responses and Th1 cell activation.[5,6] To this end, we infected WT and DAP12 KO mice and at d7 or d14 after infection, analyzed the phenotype and activation status of lung APCs. In general, there were considerably greater numbers of innate immune cells including neutrophils and

APCs (auto-fluorescence + (AF+) macrophages and AF− CD11c+CD11b+ DCs) in the lungs of infected DAP12 KO animals at d7 than in WT controls (**Supplementary Figure S3**). At d14 after infection, the frequencies of activated MHCII^{low}-expressing AF+CD11c+ macrophages (Gr1−) were also significantly greater in the lungs of DAP12 KO animals than in the WT controls (**Figure 3a**). There was an increased level of major histocompatibility complex class II (MHC II) expression on these APCs as indicated by increased mean fluorescence intensity of MHC II molecules (**Figure 3a**). Similarly, we found higher frequencies of MHC II^{high}-expressing AF−CD11c+ DCs (Gr1−) in the lungs of DAP12 KO mice compared with WT controls (**Figure 3b**). These data suggest that DAP12 pathway mediates delayed Th1 immune activation likely via regulating the activation status of APCs in the lung.

Role of DAP12 in upregulation of IRAK-M expression and downregulation of NF-κB activation in infected APCs

To understand the molecular mechanisms by which DAP12 regulates the activation status of APCs, we examined the levels of IRAK-M expression in infected APCs. IRAK-M, a member of

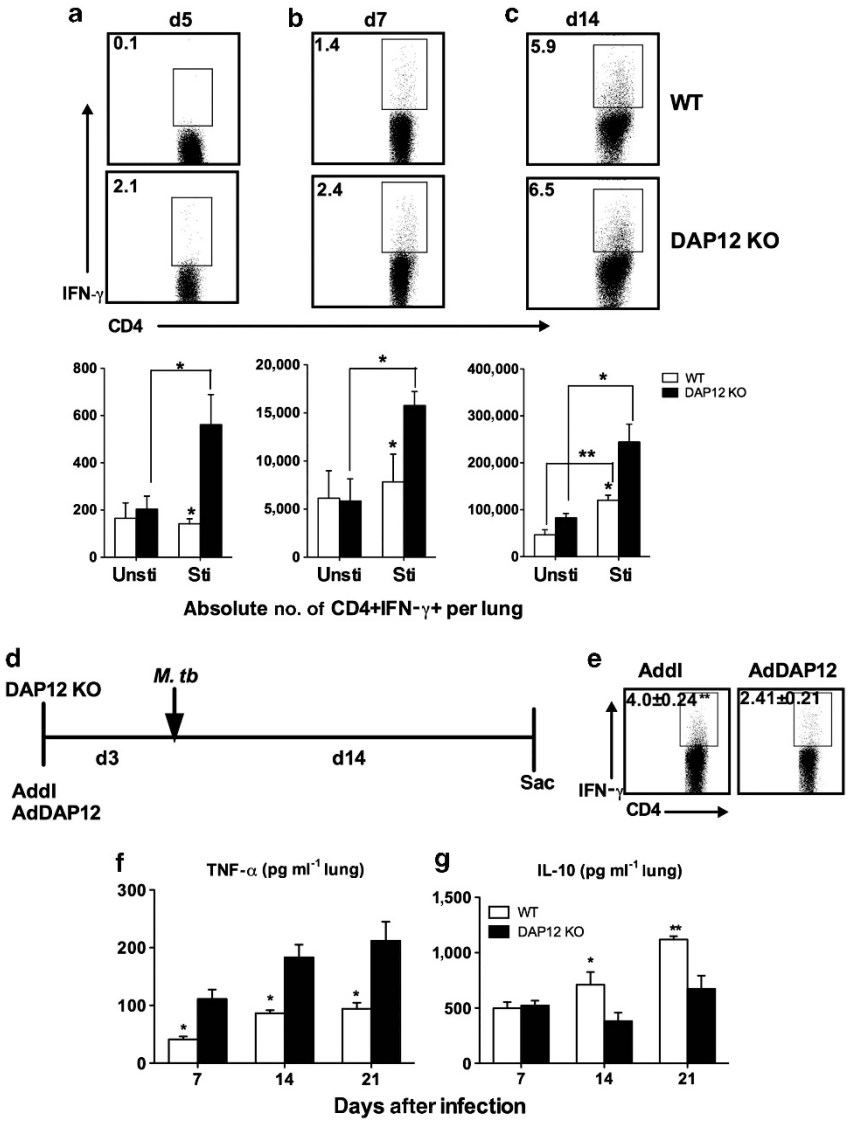

Figure 2 Mycobacterial infection delays T helper type 1 (Th1) cell responses and suppresses proinflammatory responses via DAP12 (DNAX-activating protein of 12 kDa) pathway. Lung cells were isolated and stimulated at days 5 (d5), 7 (d7), and 14 (d14) after infection with *Mycobacterium tuberculosis* (*M. tb*) from wild-type (WT) and DAP12 knockout (KO) mice and subject to immunostaining. Representative dot plots showing frequencies and absolute numbers of CD4+ interferon-γ-positive (IFN-γ+) cells in the lung at (**a**) d5, (**b**) d7, and (**c**) d14 are presented. Sti, stimulated; Unsti, unstimulated. (**d**) Experimental schema of reconstitution of DAP12 using AdDAP12 in DAP12 KO mice. (**e**) Lung cells isolated 14 days after infection from DAP12 KO mice receiving either AddI or AdDAP12 were subject to immunostaining. Representative dot plots depict frequencies of CD4+ IFN-γ+ cells in the lung. The data are expressed as mean ± s.e.m. of cell numbers from three to four mice per group, representative of more than two independent experiments. Lung homogenates from WT and DAP12 KO mice at d7 or d14 or d21 after infection were measured for (**f**) tumor necrosis factor-α (TNF-α) and (**g**) interleukin-10 (IL-10) by enzyme-linked immunosorbent assay (ELISA). Results are expressed as mean ± s.e.m. of cytokine levels from three mice per group, representative of two independent experiments. $^{*}P<0.05$, $^{**}P<0.01$.

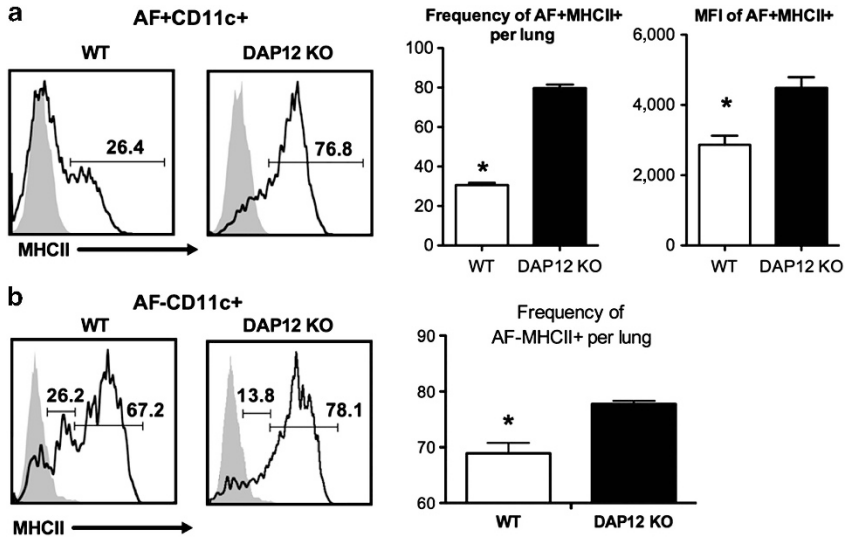

Figure 3 Mycobacterial infection suppresses antigen-presenting cell (APC) activation via DAP12 (DNAX-activating protein of 12 kDa) pathway. At day 14 (d14) after infection with *Mycobacterium tuberculosis* (*M. tb*), lung cells from wild-type (WT) and DAP12 knockout (KO) mice were immunostained for CD45, Gr1, CD11c, CD11b, and major histocompatibility complex class II (MHC II) surface markers and analyzed by flow cytometry. (**a**) auto-fluorescence + (AF +) and (**b**) AF − cells were characterized based on CD11c and MHC II expression. Representative histograms of MHC II expression by AF + and AF − CD11c + cells are shown and the bar graphs represent the mean ± s.e.m. of frequencies of MHCII + AF + CD11c + or MHCII + AF − CD11c + cells per lung and the level of MHC II expression assessed as the mean fluorescence intensity (MFI) from three to four mice per group. $^*P<0.05$.

IRAK kinase family, is induced in APCs upon Toll-like receptor stimulation and it negatively regulates Toll-like receptor signaling.[41,42] The observed heightened proinflammatory cytokine responses in infected DAP12 KO animals (**Figure 2f,g**; **Supplementary Figures S1** and **S2**) supports DAP12-mediated regulation of IRAK-M signaling pathway. To address whether this was the case, APCs (macrophages and DCs) were purified from the lungs of naive WT and DAP12 KO mice and infected with *M. tb*. Using immunofluorescent confocal microscopy, we found that although DAP12-competent WT APCs displayed markedly upregulated IRAK-M protein expression as early as 1 h after infection and remained elevated at least until 48 h (**Figure 4a,b**), the APCs deficient in DAP12 had little IRAK-M expression at 1 h after infection and the levels of IRAK-M expression somewhat increased by 2 h but remained much lower than in WT counterparts throughout (**Figure 4a,b**). To verify whether IRAK-M protein expression was also dysregulated *in vivo* because of DAP12 deficiency, we elected to examine its expression in APCs isolated at d14 after *in vivo* infection by confocal microscopy. In keeping with the above *in vitro* observations, a significantly greater number of DAP12-competent WT APCs from *in vivo*-infected lungs were found to express IRAK-M compared with those isolated from infected DAP12 KO animals (**Figure 4c**).

As it is known that IRAK-M negatively regulates Toll-like receptor activation-mediated signaling events such as nuclear factor-κB (NF-κB) nuclear translocation via inhibiting IRAK-1 phosphorylation,[41,42] by using western blot we examined the protein concentration of phospho-IRAK-1 in *in vitro*-infected APCs. In line with their heightened IRAK-M expression (**Figure 4a,b**), the WT APCs had lower levels of phospho-IRAK-1 protein (76 kDa) both at the baseline and upon infection, compared with DAP12 KO cells (**Figure 4d**). We next examined the kinetics of NF-κB nuclear translocation in infected APCs. Indeed, consistent with their heightened IRAK-M expression and decreased IRAK-1 phosphorylation, the DAP12-competent WT APCs displayed a limited extent of NF-κB nuclear translocation between 1 and 2 h in response to infection (**Figure 4e**). On the other hand, in agreement with their much reduced IRAK-M expression and heightened IRAK-1 phosphorylation, DAP12 KO APCs had much increased NF-κB nuclear translocation between 1 and 2 h that continued to intensify up to 48 h after infection (**Figure 4e**). The above data together suggest that mycobacterial infection inhibits the activation of APCs via DAP12-mediated activation of the negative regulatory IRAK-M signaling pathway.

DAP12-mediated IL-10 production and its regulation by IRAK-M in infected APCs

We have observed DAP12-mediated suppression of proinflammatory cytokine and APC responses to be correlated with increased anti-inflammatory IRAK-M and IL-10 responses (**Figures 2f,g, 3,** and **4**). Although it has recently been shown that DAP12 can upregulate IRAK-M and IL-10 expression in hepatic APCs,[32] it remains unclear whether DAP12 regulates IL-10 production and what is its relationship to IRAK-M in mycobacterium-infected APCs in the lung. To this end, we first examined IL-10 expression in APCs isolated from the lungs of WT and DAP12 KO mice infected with mycobacteria for 7 days. In accord with increased IL-10 protein in the lung of infected DAP12-competent WT animals (**Figure 2g**), infected

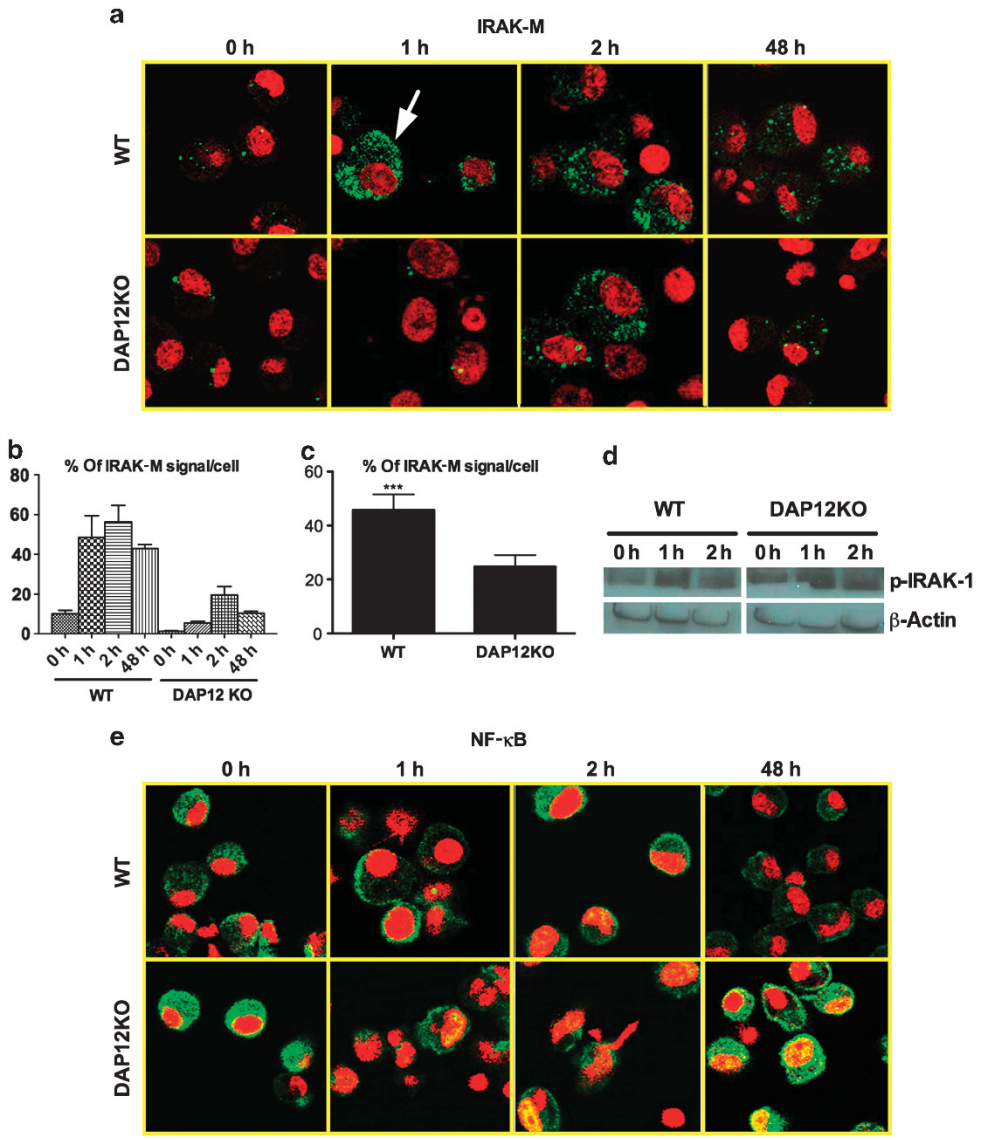

Figure 4 Mycobacterial infection induces IRAK-M (interleukin-1 receptor-associated kinase M) but decreases nuclear factor-κB (NF-κB) activation in antigen-presenting cells (APCs) via DAP12 (DNAX-activating protein of 12 kDa) pathway. (**a**) Representative confocal micrographs of kinetic IRAK-M expression at 0, 1, 2, and 48 h after *Mycobacterium tuberculosis* (*M. tb*) infection in APCs. (**b**) Semiquantification of the strength of IRAK-M signal on per-cell basis was performed using ImageJ image processing program and shown as mean ± s.e.m. of signal strength ratio of green signal (IRAK-M) to red signal (nucleus). Signal strength in 100 cells was included per condition. (**c**) APCs purified from the lungs of wild-type (WT) and DAP12 knockout (KO) mice (d14) were immunostained for IRAK-M and analyzed by confocal microscopy. Semiquantification of the strength of IRAK-M signal on per-cell basis was performed using ImageJ image program and shown as mean ± s.e.m. of signal strength ratio of green signal (IRAK-M) to red signal (nucleus). (**d**) Representative immunoblots of kinetic changes of phosphorylated IRAK-1 in infected APCs. (**e**) Representative confocal micrographs of kinetic NF-κB activation indicated by cytoplasm to nucleus translocation in infected APCs. All of the above data are representative of two independent experiments. ***$P<0.001$.

WT APCs produced significant levels of IL-10 (**Figure 5a**). In contrast, the APCs deficient in DAP12 barely produced any IL-10 (**Figure 5a**), in keeping with decreased IL-10 in the lungs of DAP12 KO animals (**Figure 2g**). To further understand the nature of IL-10-producing APC populations, we immunophenotyped these cells and examined their IL-10 expression by intracellular cytokine staining, based on their relative surface expression of CD11c and CD11b and divided them into three distinct APC populations ($CD11c^{hi}CD11b^{med}$, $CD11c^{med}CD11b^{hi}$, and $CD11c\text{-}CD11b^{med}$) in the lungs of WT and DAP12 KO mice in the early phase of mycobacterial infection (**Figure 5b**). Consistent with the observation following *ex vivo* culture (**Figure 5a**), DAP12-competent WT lungs had high frequencies of IL-10-producing APC populations, particularly the IL-10-producing $CD11c^{hi}CD11b^{med}$ and $CD11c\text{-}CD11b^{med}$ cells, whereas DAP12-deficient counterparts had significantly reduced IL-10-producing $CD11c^{hi}CD11b^{med}$ and $CD11c\text{-}CD11b^{med}$ APCs (**Figure 5b,c**).

To further examine the role of DAP12 in regulating APC IL-10 production, before infection DAP12 KO mice were reconstituted in the lung for DAP12 expression by using a viral-based gene transfer vector expressing transmembrane DAP12

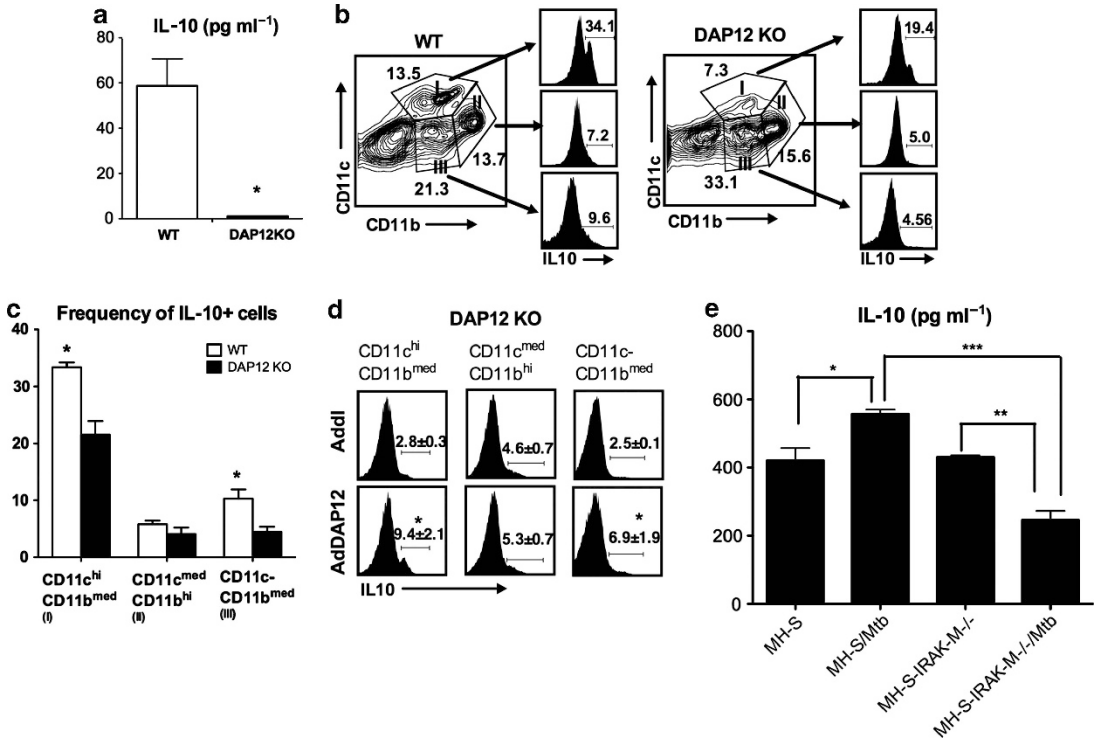

Figure 5 DAP12 (DNAX-activating protein of 12 kDa)-mediated interleukin-10 (IL-10) production is regulated by IRAK-M (interleukin-1 receptor-associated kinase M) in infected antigen-presenting cells (APCs). (**a**) At day 14 (d14) after mycobacterial infection, lung mononuclear cells isolated from wild-type (WT) and DAP12 knockout (KO) mice were cultured and supernatants were measured for IL-10 by enzyme-linked immunosorbent assay (ELISA). (**b**) Cultured cells were immunostained for CD45, Gr1, CD11c, CD11b, and intracellular IL-10, and analyzed by flow cytometry. Representative contour plots showing three subtypes of APCs: $CD11c^{hi}CD11b^{med}$ (I), $CD11c^{med}CD11b^{hi}$ (II), and CD11c-$CD11b^{med}$ (III). Histograms represent the percentage of APCs producing IL-10 in each subtype. (**c**) The frequencies of $CD11c^{hi}CD11b^{med}$ (I), $CD11c^{med}CD11b^{hi}$ (II), and CD11c-$CD11b^{med}$ (III) cell populations that produced IL-10, representing the mean ± s.e.m. from three to four mice per group. (**d**) Lung mononuclear cells isolated at d14 after infection from DAP12KO mice receiving either Addl or AdDAP12 were stimulated and immunostained as above. Histograms represent the percentage of APCs producing IL-10 in each subtype. (**e**) Bar graph representing mean ± s.e.m. IL-10 production by infected MH-S cells transfected with scrambled small interfering RNA (siRNA) or IRAK-M siRNA. Data are representative of two independent experiments. $^{*}P<0.05$, $^{**}P<0.01$, $^{***}P<0.001$.

(AdDAP12) as described in **Figure 2d**. The control DAP12 KO animals received only the control vector (Addl). The IL-10 production capacity of lung APC populations was examined d14 after infection by immunostaining the cultured mononuclear leukocytes for APC surface markers and intracellular IL-10 cytokine. Indeed, DAP12 reconstitution significantly increased the frequencies of IL-10-producing $CD11c^{hi}$ $CD11b^{med}$ and CD11c-$CD11b^{med}$ APCs in the lung (**Figure 5d**). These data indicate that DAP12 pathway plays a critical role in mycobacterial infection-induced IL-10 production in APC populations.

As we have observed DAP12-mediated IRAK-M induction in infected APCs (**Figure 4a–c**), we next sought to investigate whether upregulated IRAK-M expression was causally linked to increased IL-10 production in the APCs (**Figure 5b–d**). A recent report shows the involvement of IRAK-M in IL-10 release by lipopolysaccharide-tolerized bone marrow APCs.[43] To address this issue, we utilized a small interfering RNA (siRNA) knockdown approach and an alveolar macrophage cell line-based culture model of intracellular infection.[44] Thus, MH-S alveolar macrophages were transfected with scramble siRNA or IRAK-M-specific siRNA under optimized conditions and plated in tissue culture plates for 24 h. Cells were then infected with *M. tb* at a multiplicity of infection (MOI) of 5 for 24 h or left uninfected. An effective 70–80% reduction in IRAK-M expression was verified by quantitative PCR (data not shown). We found that IRAK-M knockdown did not significantly affect IL-10 production in uninfected macrophages (MH-S vs. MH-S-IRAK-M −/−) (**Figure 5e**). Mycobacterial infection significantly increased IL-10 production by these cells (**Figure 5e**). However, IRAK-M knockdown significantly reduced IL-10 production by infected macrophages by >50% (MH-S/Mtb vs. MH-S-IRAK-M −/−/Mtb; **Figure 5e**). The above data together suggest that mycobacterial infection induces IL-10 production in APCs via DAP-12-mediated activation of IRAK-M.

DAP12-mediated IL-10 production by infected APCs is critical to the negative regulation of Th1 cell responses in the lung

Our results thus far have identified that mycobacterial infection inhibits the activation of APCs in the lung via DAP12-mediated upregulation of IRAK-M and IL-10 in APCs, resulting in slow-developing Th1 cell responses in the lung. To further examine the role of APC-expressed DAP12 in delayed Th1 cell responses

to mycobacterial infection in the lung, we undertook an *in vivo* adoptive APC transfer approach. This approach would allow us to specifically address whether the DAP12 expressed on APCs was critical to the pace of Th1 cell development following infection, as besides APCs, other innate immune cells may also express DAP12.[21,22] To this end, WT and DAP12 KO mice were infected with *M. tb* and at d14 after infection, CD11c+ APCs were isolated and purified from the lungs, and the DAP12-competent WT APCs were adoptively transferred intratracheally to DAP12 KO mice that had been infected for 6 days (DAP12 KO-WT-APCs). As comparisons, infected WT and DAP12 KO mice were treated with no APC transfer or

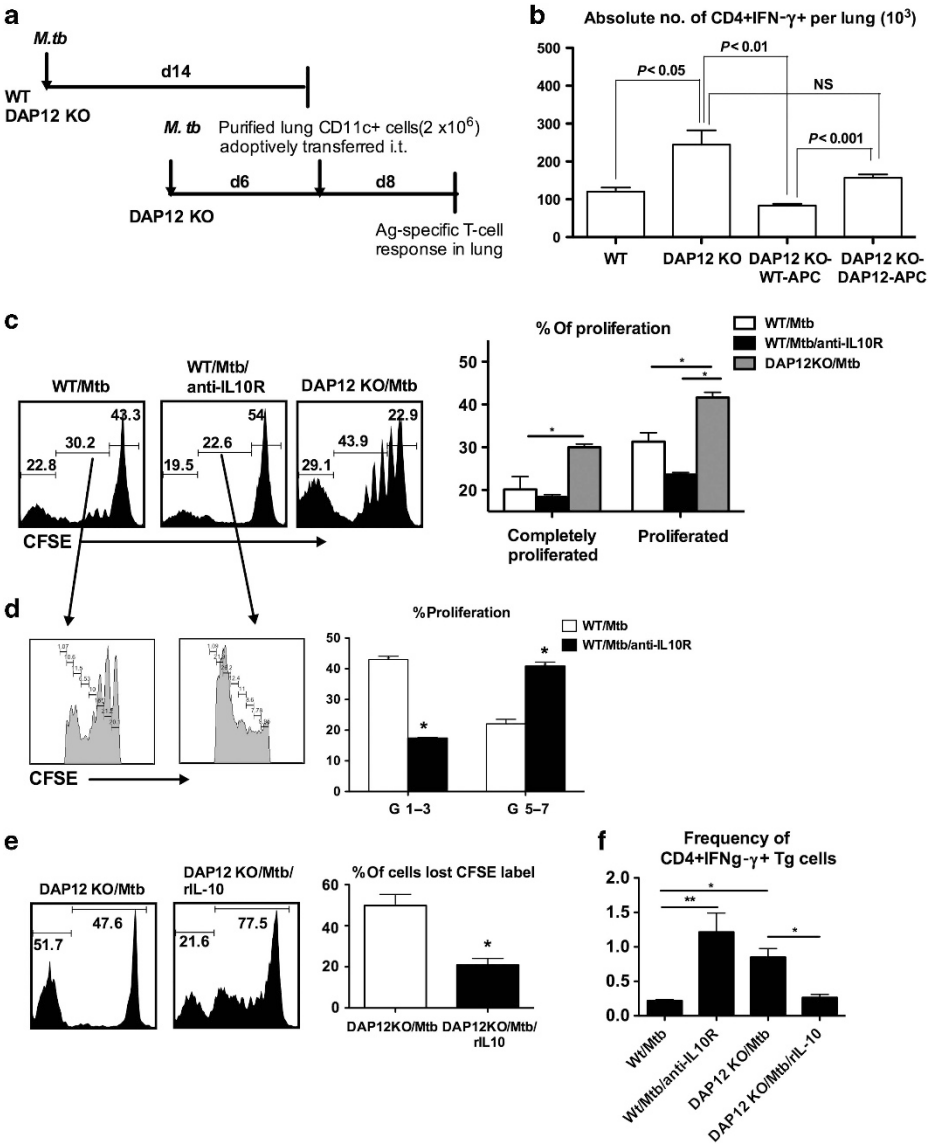

Figure 6 DAP12 (DNAX-activating protein of 12 kDa)-mediated interleukin-10 (IL-10) production by infected antigen-presenting cells (APCs) delays T helper type 1 (Th1) cell responses. (**a**) Experimental schema; i.t., intratracheal. (**b**) Bar graph showing absolute numbers of interferon-γ-positive (IFN-γ+) CD4 T cells in the lungs of wild-type (WT), DAP12 knockout (KO) mice, or DAP12 KO mice receiving either WT-APCs or DAP12KO-APCs. Data are mean ± s.e.m. from three to four mice per group, representative of two independent experiments. NS, not significant. (**c**) Mycobacterium-infected APCs from the lung of naive WT (WT/Mtb) were co-cultured with carboxyfluorescein succinimidyl ester (CFSE)-labeled transgenic (Tg) cells in the presence or absence of anti-IL-10R antibody (WT/Mtb/anti-IL10R). Infected APCs from the lung of naive DAP12 KO mice were co-cultured with CFSE-labeled Tg cells (DAP12 KO/Mtb). Representative histograms showing CFSE dilution in Tg cells after 72 h of culture. Bar graph represents mean ± s.e.m. of frequencies of cells that completely lost their CFSE labeling (completely proliferated) or those in the process of proliferation (proliferated). (**d**) Dilution of CFSE in the "proliferated" cells shown in **c** is magnified, showing frequencies of cells in each proliferation round. (**e**) Infected APsC from the lungs of naive DAP12KO mice co-cultured with CFSE-labeled Tg cells in the absence (DAP12KO/Mtb) or presence of recombinant (r)IL-10 (DAP12KO/Mtb/rIL-10). Representative histograms and bar graph show mean ± s.e.m. of frequencies of Tg cells proliferated after 96 h of culture. (**f**) Infected APCs from the lung of naive WT or DAP12KO mice co-cultured with Tg cells in the absence (DAP12KO/Mtb) or presence of rIL-10 (DAP12KO/Mtb/rIL-10). Bar graph represents mean ± s.e.m. of frequencies of Tg cells producing IFN-γ after 30 h of culture. $^{*}P<0.05$, $^{**}P<0.01$.

infected DAP12 KO mice were treated by intratracheal transfer of the DAP12-deficient APCs (DAP12 KO-DAP12 KO-APCs; **Figure 6a**). The mice were killed and the magnitude of Th1 responses in the lung was compared at 14 days after infection (8 days after APC transfer). Consist with the earlier observations (**Figure 2a**), DAP12 KO hosts had much greater levels of Th1 cell responses in the lung compared with their WT counterparts (**Figure 6b**). However, such heightened Th1 cell responses in the lungs of DAP12-deficient animals were significantly reduced by the DAP12-competent APCs adoptively transferred to the lung (DAP12 KO-WT-APCs; **Figure 6b**), in contrast to minimally altered T-cell responses in the lungs of DAP12 KO animals receiving the DAP12-deficient APCs (DAP12 KO-DAP12 KO-APCs; **Figure 6b**). These data suggest that DAP12-expressing APCs play a critical role in negatively regulating Th1 cell responses to pulmonary mycobacterial infection.

As we have observed increased and decreased IL-10 production by mycobacterial infection of DAP12-competent and -deficient APCs, respectively (**Figure 5**), which correlated inversely with the pace and magnitude of Th1 cell activation in the lung (**Figure 2**), we next examined whether infected DAP12-competent APCs negatively regulated Th1 cell activation via IL-10. In this regard, we adopted an *ex vivo* APC and T-cell co-culture model system where the APCs isolated from the lungs of naive WT (WT/Mtb) and DAP12 KO (DAP12 KO/Mtb) animals were infected *in vitro* with *M. tb* and co-cultured with carboxyfluorescein succinimidyl ester (CFSE)-labeled P25TCR-Tg (P25-Tg) CD4 T cells, specific for the peptide 25 (amino acids 240–254) of *M. tb* antigen 85B.[10] The role of infected APC-derived IL-10 in the activation of P25-Tg T cells was investigated by using an anti-IL-10R antibody added to WT APCs and P25-Tg T-cell co-cultures (WT/Mtb/anti-IL-10R) or recombinant IL-10 (rIL-10) protein added to DAP12 KO APCs and P25-Tg T-cell co-cultures (DAP12 KO/Mtb/rIL-10). The extent of CFSE dilution in the labeled P25-Tg T cells was analyzed and used as an index of Th1 cell activation in conjunction with assessment of IFN-γ-producing P25-Tg T cells. In support of the *in vivo* data (**Figure 6b**), DAP12-competent WT APCs (WT/Mtb) stimulated T cells proliferated to a significantly lesser degree than their DAP12-deficient counterparts (DAP12 KO/Mtb), with the former inducing 22% T cells of "completely proliferated" and 30% T cells of actively "proliferated," vs. DAP12 KO/Mtb APC inducing 29% "completely proliferated" and 43% "proliferated" (**Figure 6c**). Moreover, compared with WT/Mtb, although blockade of IL-10 receptor (IL-10R) signaling in T cells in WT APCs and P25-Tg T cell co-cultures (WT/Mtb/anti-IL-10R) did not increase the overall percentage of P25-Tg T-cell proliferation (22 + 30% WT/Mtb vs. 19 + 22% WT/Mtb/anti-IL10R; **Figure 6c**), blockade of IL-10R signaling in T cells (WT/Mtb/anti-IL-10R) significantly increased the T cells that had undergone 5–7 rounds of proliferation (**Figure 6d**). On the other hand, reconstitution of IL-10 levels in DAP12 KO APCs and P25-Tg T-cell co-cultures (DAP12 KO/Mtb/rIL-10) significantly reduced the extent of T-cell proliferation (**Figure 6e**). In agreement with changes in P25-Tg T-cell proliferation, DAP12 KO APCs (DAP12 KO/Mtb) significantly increased the frequency of IFN-γ + Tg CD4 T cells compared with WT APCs (Wt/Mtb; **Figure 6f**). Blockade of IL-10 signaling in WT APC-Tg cell co-cultures (WT/Mtb/anti-IL-10R) significantly increased the frequency of IFN-γ + Tg T cells, whereas introduction of exogenous rIL-10 to the co-culture with DAP12 KO APCs (DAP12 KO/Mtb/rIL-10) markedly reduced such T cells (**Figure 6f**). These data together indicate that DAP12 pathway negatively regulates Th1 cell activation via its inducing effect on APC IL-10 production.

Mycobacterial infection inhibits Ag presentation and Th1 cell activation in the dLNs via DAP12-regulated APC IL-10 production

The above observations establish that mycobacterium-infected APCs negatively regulate Th1 cell responses in the lung via the DAP12-regulated IRAK-M and IL-10 pathways, thus resulting in delayed expression of protective Th1 immunity in the lung. As it is known that the initiation of Th1 cell activation occurs in the local dLNs following mycobacterial infection,[10] we next examined whether the observed delayed Th1 cell responses in the lungs of DAP12-competent WT hosts resulted from suppressed Ag-specific Th1 cell priming in the dLNs and its relationship with DAP12-regulated APC IL-10 expression. To this end, we first compared the capacity of IL-10 production by the APCs in the dLNs of WT and DAP12 KO mice at d7 and d10 after infection. Purified CD11c + APCs were cultured in the presence of *M. tb*-specific Ag, and IL-10 levels in the culture supernatants were measured by enzyme-linked immunosorbent assay (ELISA). The DAP12-competent APCs isolated from the dLNs of infected WT mice at d7 or d10 produced high amounts of IL-10 (**Figure 7a**). In stark contrast, lack of DAP12 in the APCs resulted in significantly diminished IL-10 production at the both time points (**Figure 7a**). The above data together suggest that mycobacterial infection renders APC immune suppression not only in the lungs but also in the dLNs via DAP12 pathway. To examine whether this could have affected mycobacterial Ag presentation and Th1 cell priming in the dLNs, we utilized an *in vivo* approach to examine Ag presentation and T-cell activation whereby CFSE-labeled P25 transgenic (P25-Tg) CD4 T cells specific for *M. tb* Ag85B antigen were adoptively transferred intravenously to WT, DAP12 KO, and IL-10 KO mice. It was subsequently found that transferred P25-Tg CD4 T cells populated the lung dLNs of three strains of mice at an equal rate (~1%; data not shown). The mice were infected with mycobacteria at 1 day after adoptive T-cell transfer, and at 10 days after infection, the dLNs were harvested and the levels of P25-Tg CD4 T-cell activation were assessed by fluorescence-activated cell sorting (FACS) analysis of the extent of Ag-stimulated P25-Tg T-cell proliferation (**Figure 7b**). In all three strains of mice, P25-Tg CD4 T cells in the dLNs had undergone 1 to 6 rounds of proliferation (**Figure 7c**). However, compared with the T cells in the dLNs of WT hosts, significantly more P25-Tg

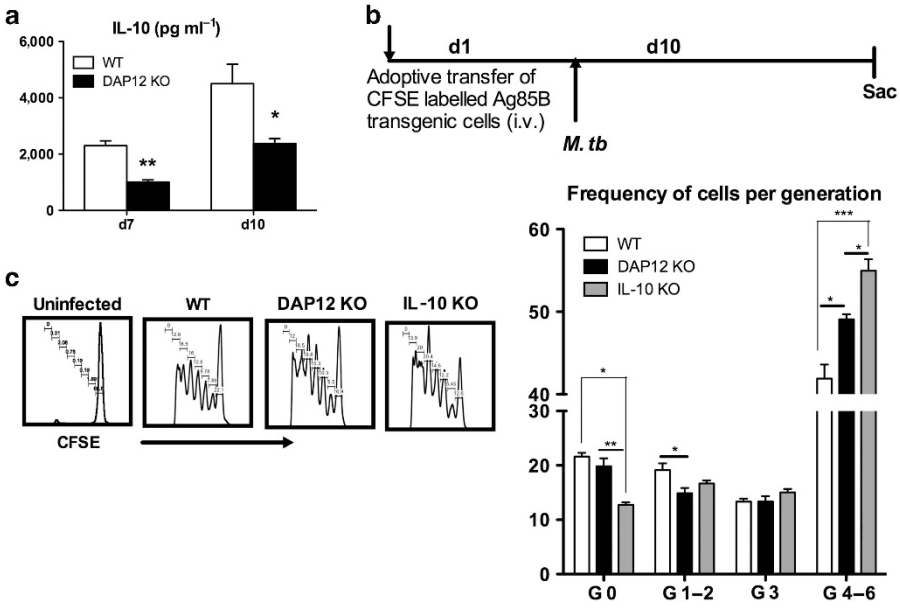

Figure 7 DAP12 (DNAX-activating protein of 12 kDa)-induced interleukin-10 (IL-10) producing antigen-presenting cells (APCs) inhibits antigen (Ag) presentation and T helper type 1 (Th1) cell activation in draining lymph nodes (dLNs). (**a**) Purified APCs from dLNs of wild-type (WT) and DAP12 knockout (KO) mice at days 7 (d7) and 10 (d10) after infection (*M.tb*H37Ra) were stimulated for 48 h and IL-10 was measured in the supernatants by enzyme-linked immunosorbent assay (ELISA). Data represent mean ± s.e.m. of triplicate samples, representative of two independent experiments. (**b**) Experimental schema; i.v., intravenous. (**c**) Representative histograms showing carboxyfluorescein succinimidyl ester (CFSE) dilution in transferred transgenic (Tg) cells in infected WT, DAP12 KO, and IL-10 KO mice. Bar graph represents mean ± s.e.m. of frequencies of Tg cells at various generations (G) of proliferation. $^{*}P<0.05$, $^{**}P<0.01$, $^{***}P<0.001$.

T cells in the dLNs of DAP12-deficient hosts had undergone up to 4–6 rounds of proliferation, similar to the proliferation profile seen in the dLNs of IL-10-deficient hosts (**Figure 7c**). These data indicate that similar to the APCs in the lung, mycobacterial infection also renders the APCs in the dLNs to be immune-suppressed and produce increased IL-10 production via DAP12 pathway, which results in reduced Ag-specific Th1 cell priming in the dLNs and subsequently delayed Th1 cell responses in the lung.

DISCUSSION

It has increasingly been recognized that compared with other intracellular respiratory pathogens, *M. tb* is adept at manipulating the host defense's machinery including retarding T-cell activation to favor its establishment and persistence in the lung.[7,8,12–15] Currently, this is believed to be an important reason for high prevalence of latent infection in humans. Unfortunately, the cellular and molecular immune mechanisms underlying retarded induction of Th1 immunity following lung mycobacterial infection still remain poorly understood despite some recent progress.[16–19] In this study we have identified a novel molecular pathway operating in APCs that involves the DAP12/IRAK-M/IL-10 axis and plays an important role in delaying Th1 immunity to *M. tb* infection. We find that on infection of APCs, DAP12 controls the activation of APCs in the lung via upregulating IRAK-M that then causes increased IL-10 production. On the other hand, increased IRAK-M decreases IRAK-1 phosphorylation that leads to reduced NF-κB nuclear translocation. These changes suppress APC activation. Such immune-suppressed APsC by mycobacterial infection leads to delayed Th1 cell responses in the dLNs and the lung in the early course of infection. This in turn results in compromised immune protection (**Supplementary Figure S4**—a schematic illustration of the mechanistic model).

Given the critical instructing role of APCs in T-cell activation and the tropism of mycobacteria for APCs, APCs is believed to be an important focal point at which mycobacterial infection manipulates the mechanisms of host defense. Although a number of studies have found that mycobacterial infection increases the production of immune-suppressive IL-10 from APCs, thus causing an immune-suppressed phenotype of APCs with reduced T cell-activating capability,[10,19,38,40,45,46] the molecular pathways remain poorly defined. Our current findings point to a key role of mycobacterium-altered functionality of APCs via the DAP12/IRAK-M/IL-10 pathway in delaying Th1 cell priming in dLNs and their subsequent recruitment to the lung. The delayed lung recruitment of Th1 cells most likely results from impaired T-cell priming and chemokine responses in the lung. Indeed, we have found that compared with DAP12-deficient animals, the DAP12-competent animals not only suffer diminished levels of proinflammatory cytokines such as TNF-α but also lymphocytic chemokines including RANTES (regulated on activation, normal T cell expressed and secreted) and IP-10 in the lung in the early course of infection (data not shown). Both RANTES and IP-10 were shown to play a role in pathogen-experienced T-cell homing to the lung.[47,48]

Recent emerging evidence suggests that the delayed Th1 emergence in the lung is common to infection by the slow-growing mycobacterial species including *M. tb*, *M. bovis* BCG, and Mycobacterium *avium*, independent of their relative virulence and doses of exposure.[10,11,14,15,49,50] In this regard, in this study we indeed found that the Th1 cell response was also significantly delayed following infection with *M.tb*H37Ra, which was associated with delayed lung protection, as it would be following *M.tb*H37Rv infection. This phenomenon is likely attributed to the robust immune-suppressive property of the cell wall component mannose-capped lipoarabinomannan that is associated with only the slow-growing mycobacterial species, but not the fast-growing species such as Mycobacterium *smegmatis*.[51] Indeed, mannose-capped lipoarabinomannan was found to attenuate macrophage activation via inducing IRAK-M.[52] As we have identified a mechanistic linkage between DAP12, IRAK-M, and IL-10 in infected APCs in this study, whether mycobacterial mannose-capped lipoarabinomannan may directly interact with DAP12-associated, nonsignaling but ligand-binding receptors such as TREM-2 (**Supplementary Figure S4**)[21,22,26,28] is an interesting question that warrants an independent investigation in future.

In support of our current findings, recent screening of immune mediators associated with TB has revealed an association of higher levels of IRAK-M and IL-10 with decreased innate and Th1 immunity in the sputum samples of TB patients.[53] IL-10 has also been correlated with increased susceptibility to TB in humans.[54,55] Thus, our findings that mycobacterial infection exploits the DAP12/IRAK-M/IL-10 pathway to inhibit the function of APCs and, subsequently, Th1 cell activation suggest the potential of immunologically targeting DAP12, IRAK-M, and/or IL-10 for improved efficacy of BCG vaccination or TB chemotherapy in humans. In this regard, the blocking agents targeting DAP12 pathway could be potentially employed.[56] In this study, we have used siRNA to knock down IRAK-M expression in APCs for enhanced activation in infected APCs. The siRNA knockdown of IRAK-M has also been shown to strengthen the potency of DC vaccines by enhancing their Ag-presenting function and migration.[57] Furthermore, nitrogen bisphosphonates commonly prescribed for treating osteoporosis have recently been shown to target IRAK-M. Thus, nitrogen bisphosphonate was found to enhance both cellular and antibody responses to antigens.[58] On the other hand, we have shown herein that use of anti-IL-10R reversed the mycobacterium-imposed immune-suppressive phenotype of APCs for enhanced T-cell activation, thus supporting the notion that treatment with anti-IL-10R antibodies holds great potential for immune-modulating strategies to enhance protection against human pathogens.[59]

In summary, our study has identified a novel DAP12/IRAK-M/IL-10 mechanistic pathway in APCs that tuberculous infection utilizes to lead to delayed induction of Th1 immunity in the lung. Engagement of this pathway causes suppressed NF-κB activation, reduced proinflammatory cytokines and chemokines, and decreased capability of APCs to activate Th1 cells. The findings hold implications in the development of TB vaccination and immunotherapeutic strategies.

METHODS

Mice. The breeding colony of DAP12-gene knockout (DAP12 KO) mice fully backcrossed to the C57BL/6 genetic background is maintained in the central animal facility at McMaster University. Age- and sex-matched wt C57BL/6 control mice were purchased from Harlan (Indianapolis, IN). Age- and sex-matched B6 background IL-10 KO mice (B6.129P2-*Il10tm1Cgn*/J) and C57BL/6-Tg (H2-Kb-Tcra,-Tcrb) P25Ktk/J transgenic mice were purchased from Jackson Laboratories (Bar Harbor, ME). Male mice were used and were housed in the specific pathogen-free facility. All experiments were conducted in accordance with the guidelines of animal research ethics board of McMaster University.

***M. tb* preparation and infection**. *M. tb* bacilli were grown in Middlebrook 7H9 broth (Sigma-Aldrich, Oakville, ON, Canada) supplemented with Middlebrook oleic acid–albumin–dextrose–catalase enrichment, 0.002% glycerol, and 0.05% Tween-80 for 10–15 days, aliquoted, and stored in −70 °C until needed.[60,61] Infection with the H37Rv strain was carried out by intranasal delivery of bacilli (10^4 CFU) and the levels of mycobacterial infection were determined in the lung and spleen by plating serial dilutions of tissue homogenates in triplicates onto Middlebrook 7H10 agar plates. Plates were incubated at 37 °C for 17 days. Colonies were then counted, calculated, and presented as $\log_{10}$ CFU per organ as previously described. Before each *in vivo* or *in vitro* use, *M. tb* bacilli were washed with phosphate-buffered saline (PBS) containing 0.05% Tween-80 twice and passed through a 27-gauge needle 10 times to disperse clumps. In the experiments where detailed immunologic analyses were carried out, the H37Ra strain was used for infection (5×10^5 CFU). The use of attenuated *M. tb*, the H37Ra strain, allowed us to carry out detailed T-cell and APC analysis, confocal microscopy, APC purification, and adoptive intratracheal and intravenous transfer of APCs or transgenic T cells to infected mice under technically much less constrained BSL2 conditions. For histopathological examination, left lungs were harvested and fixed in 10% formalin and subsequently paraffin embedded, sectioned, and hematoxylin and eosin stained.

Lung and dLN mononuclear cell and APC purification. The lungs and the mediastinal dLNs were removed aseptically. Lungs were processed to single-cell suspension by collagenase digestion as previously described. Mediastinal dLNs were processed to single-cell suspension by collagenase type II in cRPMI (1 mg ml^{-1}; Worthington Biochemical, Lakewood, NJ) with constant agitation for 60 min at 37 °C. After digestion, 20 µl of 0.5 M EDTA per ml of collagenase was added and incubated for 5 min with agitation at room temperature to disrupt T-cell–DC complexes. Whole-cell suspension was then passed through a nylon mesh filter. Cell suspension was then centrifuged at 1,500 r.p.m. for 5 min. Cell pellet was then resuspended in cRPMI-1640 with 10% fetal bovine serum, 1% L-glutamine, and 1% penicillin and streptomycin.

The purification of APCs from the lung and dLN single-cell suspensions was performed as previously described.[62] Briefly, total mononuclear cells were pooled and incubated with CD11c microbeads (Miltenyi Biotec, Auburn, CA) according to the manufacturer's instructions. CD11c-labeled cells were then passed through an MS column on the OctoMACS separator (Miltenyi Biotec). Samples were run through MACS separation columns twice to achieve higher purity. The purity of CD11c+CD11b+/− populations was consistently >90% as determined by FACS. Following CD11c+ cell separation, the negative fraction was then labeled with CD11b microbeads (Miltenyi Biotec) according to the manufacturer's instructions. The purity of CD11c−CD11b+ population was also consistently >90%. The purified CD11c+CD11b+/− and CD11c−CD11b+ subsets were then combined and used as APC preparation.

Cell culture, cell surface immunostaining, intracellular cytokine staining, and flow cytometry. Single-cell suspensions isolated from the lungs were cultured in a U-bottom 96-well plate at a concentration of 20 million cells per ml. Cells were cultured and stimulated for intracellular cytokine staining and FACS analysis as previously described.[11] Briefly, cells were cultured with or without stimulation by crude BCG and *M. tb* culture filtrate at a concentration of 1 μg per well for a total of 18 h. Golgi plug (5 μg ml^{-1} brefeldin A; BD Pharmingen, Mississauga, ON, Canada) was added to the cultures for the last 6 h of incubation. Cells were then washed and blocked with CD16/CD32 in 0.5% bovine serum albumin/PBS for 15 min on ice and immunostained with selected monoclonal antibodies. Cells were then washed, permeabilized, and stained according to the manufacturer's instructions for intracellular cytokines. The following fluorochrome-labeled monoclonal antibodies were used: CD8a-APC-Cy7, CD4-PE-Cy7, CD3-CyChrome, IFN-γ-APC, and TNF-α-PerCPeF710 (BD Pharmingen). Immunophenotyping of APC populations was performed as previously described.[62] Fluorochrome-conjugated monoclonal antibodies to CD3, CD45, CD3, Gr1, CD11c, CD11b, MHC, and class II were used for immunostaining. For intracellular IL-10, IL-12, and TNF-α production by APCs, lung mononuclear cells were cultured in the presence of cBCG and *M. tb* culture filtrate for 24 h in the presence of Golgi plug (5 μg ml^{-1} brefeldin A; BD Pharmingen) for the last 6 h of incubation. Immunostaining was performed as described above. All data were collected with the LSRII (BD Pharmingen) flow cytometer using FACSDiva software and analyzed with FlowJo software (BD Biosciences, Tree Star Inc., Ashland, OR).

NF-κB and IRAK-M immunofluorescent staining and confocal microscopy. APCs purified from the lungs (250,000/chamber) were plated on 8-chamber culture slide. Cells were infected with *M. tb* at MOI of 1 in the presence of 10 μl normal serum in a total volume of 200 μl cRPMI containing penicillin only. At various time points following infection, cells were fixed in 4% paraformaldehyde for 20 min. After washing (0.05% Tween-20 in PBS), cells were blocked with blocking buffer (5% normal goat serum, 5% bovine serum albumin, 0.1% Triton-X in PBS) for 45 min and then stained for either NF-κB (1:300; p65 rabbit polyclonal; Santa Cruz Biotechnology, Dallas, TX) or IRAK-M (1:100; Cell Signaling Technology, Danvers, MA) at room temperature for 2 h. Cells were then washed and stained with a secondary antibody (AlexaFluor 488-conjugated goat anti-rabbit; Molecular Probes, Burlington, ON, Canada) at room temperature for 1 h. After 3× washes, they were counterstained with propidium iodide (1:3,000; Molecular Probes) for 5 min before being mounted with Dako fluorescence mounting medium (Burlington, ON, Canada). Fluorescent signals were visualized using the Carl Zeiss LSM510 confocal microscope (Oberkochen, Germany) and images were generated using LSM510 image browser. Semiquantification of strength of IRAK-M signal on cell basis was performed based on the signal strength ratio of green to red signal using ImageJ (East Greenbush, NY) image processing program.

Detection of phospho-IRAK-1 by immunoblotting. APCs purified from the lungs (1 million per well) were plated on 24-well culture plate. Cells were infected with *M. tb* at MOI of 1 in the presence of 10 μl normal serum in a total volume of 200 μl cRPMI containing penicillin only. At various time points following infection, cells were trypsinized for total protein extraction. Cells were then lysed in a radioimmunoprecipitation assay buffer (1.0% Igepal CA-630, 0.5% sodium desoxycholate, 0.1% sodium dodecyl sulfate) supplemented with 1 mM sodium orthovanadate, 20 mg ml^{-1} phenylmethylsulfonyl fluoride, and a protease inhibitor cocktail (Sigma-Aldrich). Total proteins from each condition were denatured and separated by 4–20% sodium dodecyl sulfate–polyacrylamide electrophoresis that were subsequently transferred to nitrocellulose membranes (Bio-Rad, Mississauga, ON, Canada). The membranes were blotted with specific antibodies and protein expression was detected using Thermo Scientific ECL 2 (Fisher Scientific, Ottawa, ON, Canada). Rabbit anti-mouse polyclonal phospho-IRAK1 (1:500 dilution, Sigma-Aldrich) and goat anti-mouse monoclonal β-actin (1:1,000; Cell Signaling) were used as primary antibodies. Horseradish peroxidase-conjugated goat anti-rabbit IgG (1:5,000) and horseradish peroxidase-conjugated mouse anti-goat IgG (1:2,000; Santa Cruz Biotechnology) were used as secondary antibodies.

siRNA knockdown of IRAK-M expression in alveolar macrophages. An alveolar macrophage cell line (MH-S) was transfected with scramble siRNA or IRAK-M siRNA (Life Technologies, Burlington, ON, Canada) at 15 nmol each using Lipofectamine RNAiMAX reagent (Invitrogen, Burlington, ON, Canada). Briefly, the macrophages were plated in a 24-well tissue culture plate and left to rest overnight in 500 μl antibiotic-free culture medium. The next day, 100 μl of scramble siRNA or IRAK-M-specific siRNA prepared according to the manufacturer's instruction was added, and the cells were incubated for 24 h at 37 °C in 5% CO_2. After wash, cells were resuspended in 200 μl antibiotic-free culture medium and incubated for 3 h at 37 °C in 5% CO_2 and infected with *M. tb* at MOI of 5. To analyze IRAK-M mRNA expression, cells were lysed by adding RLT lysis buffer (Qiagen, Valencia, CA) according to the manufacturer's protocol. Total RNA was isolated using the RNeasy kit (Qiagen). RNA (100 ng) was reversed transcribed for each condition. Total RNA used for reverse transcription was kept constant to ensure equal RNA was used in the scramble siRNA- and IRAK-M-specific siRNA groups. The reaction mixtures were incubated at 25 °C for 5 min, 42 °C for 30 min, and 85 °C for 5 min. The expression of IRAK-M was quantified by using a PerfeCTa SYBR Green FasMix, ROX kit (Quanta Bioscience, Gaithersburg, MD) on an ABI 7900HT sequence detection system (Applied Biosystems, Foster City, CA). The expression of IRAK-M was normalized to expression of β-actin expression.

P25TCR-Tg CD4 T-cell isolation, CFSE labeling, and *in vivo* adoptive transfer. The peripheral lymph nodes and spleen were aseptically removed from P25TCR-Tg mice aged between 8 and 16 weeks, and tissues were disrupted by forcing them through a 70-μm cell strainer (BD Biosciences, Mississauga, ON, Canada) in cRPMI. CD4 T cells were magnetically isolated using a CD4 T Cell Isolation kit (Miltenyi Biotech) and an OctoMACS separator. CD4 T-cell purity was routinely >90%. For *in vitro and in vivo* proliferation assays, CD4 T cells were labeled with CFSE by resuspending the P25TCT-Tg CD4 cells at a density of 20×10^6 cells per ml in 5% fetal bovine serum/PBS containing 1 μg ml^{-1} 0.5 mM CFSE (CFDA-SE; Invitrogen). Cells were incubated with CFSE for 5 min at room temperature. Labeling was stopped with an excess of 5% fetal bovine serum/PBS and the cells were washed three times with cRPMI. For *in vivo* proliferation assay, 3–5×10^6 CFSE-labeled Ag85B-Tg cells were adoptively transferred intravenously into mice 1 day before mycobacterial challenge.

***Ex vivo* APC and P25TCR-Tg CD4 T cell co-culture**. The purified APCs (100,000 per well) were infected with *M. tb* (MOI of 1:5) and co-cultured with CFSE-labeled P25TCT-Tg CD4+ cells in a ratio of 1:2 in 96-well U-bottom plate at 37 °C and 5% CO_2 for 72 or 96 h in the presence or absence of recombinant IL-10 (40 ng ml^{-1}; R&D Systems, Minneapolis, MN) or in the presence and absence of IL-10R blocking antibody (15 μg ml^{-1}; Biolegend, Burlington, ON, Canada). Cells were then washed and immunostained for CD3 and CD4 cell surface markers and CFSE dilution in CD3+CD4+ T cells were analyzed by flow cytometry.

DAP12 gene transfer to the lung of DAP12 KO animals by using an adenoviral vector. A replication-deficient adenoviral vector expressing murine DAP12 (AdDAP12)[56] was used to reconstitute DAP12 in the lungs of DAP12 KO mice. As control, an adenoviral vector that does not contain cytokine transgene was used (Addl). A single dose of AdDAP12 or Addl vector (1×10^8 PFU) was delivered intranasally to the lung of DAP12 KO mice 3 days before mycobacterial

infection. We have previously shown that Ad-mediated gene transfer renders transgene expression locally in the lung for ~12–18 days.[63]

Analysis of cytokines in lung homogenates and cell culture supernatants. Cytokines and chemokines were measured by ELISA (R&D Systems) or Luminex (Medicorp, Montreal, QC, Canada) according to the manufacturer's protocol. The culture supernatants were collected at 60 h and stored at −20 °C until cytokine measurement.

Data analysis. Asterisk marks (*, **, and ***) indicate the differences deemed statistically significant ($P<0.05$, $P<0.01$, and $P<0.001$, respectively). A two-tailed Student's *t*-test was performed for pairwise comparisons. One-way analysis of variance analysis and the subsequent Tukey's *post hoc* test were carried out for the comparison of multiple groups. All analyses were performed using GraphPad Prism software (GraphPad Software, La Jolla, CA).

SUPPLEMENTARY MATERIAL is linked to the online version of the paper at http://www.nature.com/mi

ACKNOWLEDGMENTS

This work was supported by funds from the Canadian Institutes of Health Research. We thank Drs Toshiyuki Takai and Wayne Yokoyama for providing DAP12KO breeding mice.

DISCLOSURE

The authors declared no conflict of interest.

REFERENCES

1. WHO. Global Tuberculosis Report 2012 (2012).
2. Jeyanathan, M, Heriazon, A & Xing, Z. Airway luminal T cells: a newcomer on the stage of TB vaccination strategies. *Trends Immunol.* **31**, 247–252 (2010).
3. Ottenhoff, T.H. & Kaufmann, S.H. Vaccines against tuberculosis: where are we and where do we need to go?. *PLoS Pathog.* **8**, e1002607 (2012).
4. Flynn, J.L., Chan, J & Lin, P.L. Macrophages and control of granulomatous inflammation in tuberculosis. *Mucosal Immunol.* **4**, 271–278 (2011).
5. McCormick, S, Shaler, C.R. & Xing, Z. Pulmonary mucosal dendritic cells in T-cell activation: implications for TB therapy. *Expert Rev. Respir. Med.* **5**, 75–85 (2011).
6. Cooper, A.M. & Khader, S.A. The role of cytokines in the initiation, expansion, and control of cellular immunity to tuberculosis. *Immunol. Rev.* **226**, 191–204 (2008).
7. Chackerian, A.A., Perera, T.V. & Behar, S.M. Gamma interferon-producing CD4 + T lymphocytes in the lung correlate with resistance to infection with Mycobacterium tuberculosis. *Infect. Immun.* **69**, 2666–2674 (2001).
8. Chackerian, A.A., Alt, J.M., Perera, T.V., Dascher, C.C. & Behar, S.M. Dissemination of Mycobacterium tuberculosis is influenced by host factors and precedes the initiation of T-cell immunity. *Infect. Immun.* **70**, 4501–4509 (2002).
9. Reiley, W.W. *et al.* ESAT-6-specific CD4 T cell responses to aerosol Mycobacterium tuberculosis infection are initiated in the mediastinal lymph nodes. *Proc. Natl. Acad. Sci. USA* **105**, 10961–10966 (2008).
10. Wolf, A.J. *et al.* Initiation of the adaptive immune response to Mycobacterium tuberculosis depends on antigen production in the local lymph node, not the lungs. *J. Exp. Med.* **205**, 105–115 (2008).
11. Horvath, C.N., Shaler, C.R., Jeyanathan, M, Zganiacz, A & Xing, Z. Mechanisms of delayed anti-tuberculosis protection in the lung of parenteral BCG-vaccinated hosts: a critical role of airway luminal T cells. *Mucosal Immunol.* **5**, 420–431 (2012).
12. Cooper, A.M. T cells in mycobacterial infection and disease. *Curr. Opin. Immunol.* **21**, 378–384 (2009).
13. North, R.J. & Jung, Y.J. Immunity to tuberculosis. *Annu. Rev. Immunol.* **22**, 599–623 (2004).
14. Urdahl, K.B., Shafiani, S & Ernst, J.D. Initiation and regulation of T-cell responses in tuberculosis. *Mucosal Immunol.* **4**, 288–293 (2011).
15. Shaler, C.R., Horvath, C, Lai, R & Xing, Z. Understanding delayed T-cell priming, lung recruitment, and airway luminal T-cell responses in host defense against pulmonary tuberculosis. *Clin. Dev. Immunol.* **2012**, 628293 (2012).
16. Blomgran, R, Desvignes, L, Briken, V & Ernst, J.D. Mycobacterium tuberculosis inhibits neutrophil apoptosis, leading to delayed activation of naive CD4 T cells. *Cell Host Microbe* **11**, 81–90 (2012).
17. Divangahi, M, Desjardins, D, Nunes-Alves, C, Remold, H.G. & Behar, S.M. Eicosanoid pathways regulate adaptive immunity to Mycobacterium tuberculosis. *Nat. Immunol.* **11**, 751–758 (2010).
18. Shafiani, S, Tucker-Heard, G, Kariyone, A, Takatsu, K & Urdahl, K.B. Pathogen-specific regulatory T cells delay the arrival of effector T cells in the lung during early tuberculosis. *J. Exp. Med.* **207**, 1409–1420 (2010).
19. Wolf, A.J. *et al.* Mycobacterium tuberculosis infects dendritic cells with high frequency and impairs their function in vivo. *J. Immunol.* **179**, 2509–2519 (2007).
20. Aoki, N, Kimura, S & Xing, Z. Role of DAP12 in innate and adaptive immune responses. *Curr. Pharm. Des.* **9**, 7–10 (2003).
21. Turnbull, I.R. & Colonna, M. Activating and inhibitory functions of DAP12. *Nat. Rev. Immunol.* **7**, 155–161 (2007).
22. Lanier, L.L. DAP10- and DAP12-associated receptors in innate immunity. *Immunol. Rev.* **227**, 150–160 (2009).
23. Hamerman, J.A., Ni, M, Killebrew, J.R., Chu, C.L. & Lowell, C.A. The expanding roles of ITAM adapters FcRgamma and DAP12 in myeloid cells. *Immunol. Rev.* **232**, 42–58 (2009).
24. Bouchon, A, Facchetti, F, Weigand, M.A. & Colonna, M. TREM-1 amplifies inflammation and is a crucial mediator of septic shock. *Nature* **410**, 1103–1107 (2001).
25. Hamerman, J.A., Tchao, N.K., Lowell, C.A. & Lanier, L.L. Enhanced Toll-like receptor responses in the absence of signaling adaptor DAP12. *Nat. Immunol.* **6**, 579–586 (2005).
26. Hamerman, J.A., Jarjoura, J.R., Humphrey, M.B., Nakamura, M.C., Seaman, W.E. & Lanier, L.L. Cutting edge: inhibition of TLR and FcR responses in macrophages by triggering receptor expressed on myeloid cells (TREM)-2 and DAP12. *J. Immunol.* **177**, 2051–2055 (2006).
27. French, A.R. *et al.* DAP12 signaling directly augments proproliferative cytokine stimulation of NK cells during viral infections. *J. Immunol.* **177**, 4981–4990 (2006).
28. Turnbull, I.R. *et al.* Cutting edge: TREM-2 attenuates macrophage activation. *J. Immunol.* **177**, 3520–3524 (2006).
29. Divangahi, M. *et al.* Critical negative regulation of type 1 T cell immunity and immunopathology by signaling adaptor DAP12 during intracellular infection. *J. Immunol.* **179**, 4015–4026 (2007).
30. N'Diaye, E.N. *et al.* TREM-2 (triggering receptor expressed on myeloid cells 2) is a phagocytic receptor for bacteria. *J. Cell. Biol.* **184**, 215–223 (2009).
31. McCormick, S. *et al.* Control of pathogenic CD4 T cells and lethal immunopathology by signaling immunoadaptor DAP12 during influenza infection. *J. Immunol.* **187**, 4280–4292 (2011).
32. Sumpter, T.L., Packiam, V, Turnquist, H.R., Castellaneta, A, Yoshida, O & Thomson, A.W. DAP12 promotes IRAK-M expression and IL-10 production by liver myeloid dendritic cells and restrains their T cell allostimulatory ability. *J. Immunol.* **186**, 1970–1980 (2011).
33. Aoki, N, Zganiacz, A, Margetts, P & Xing, Z. Differential regulation of DAP12 and molecules associated with DAP12 during host responses to mycobacterial infection. *Infect. Immun.* **72**, 2477–2483 (2004).
34. Cooper, A.M. Cell-mediated immune responses in tuberculosis. *Annu. Rev. Immunol.* **27**, 393–422 (2009).
35. Wakeham, J, Wang, J & Xing, Z. Genetically determined disparate innate and adaptive cell-mediated immune responses to pulmonary Mycobacterium bovis BCG infection in C57BL/6 and BALB/c mice. *Infect. Immun.* **68**, 6946–6953 (2000).
36. Zganiacz, A. *et al.* TNF-alpha is a critical negative regulator of type 1 immune activation during intracellular bacterial infection. *J. Clin. Invest.* **113**, 401–413 (2004).
37. de la Barrera, S. *et al.* IL-10 down-regulates costimulatory molecules on Mycobacterium tuberculosis-pulsed macrophages and impairs the lytic activity of CD4 and CD8 CTL in tuberculosis patients. *Clin. Exp. Immunol.* **138**, 128–138 (2004).

38. Redford, P.S. *et al.* Enhanced protection to Mycobacterium tuberculosis infection in IL-10-deficient mice is accompanied by early and enhanced Th1 responses in the lung. *Eur. J. Immunol.* **40**, 2200–2210 (2010).
39. Redford, P.S., Murray, P.J. & O'Garra, A. The role of IL-10 in immune regulation during M. tuberculosis infection. *Mucosal Immunol.* **4**, 261–270 (2011).
40. Shaler, C.R. *et al.* Pulmonary mycobacterial granuloma increased IL-10 production contributes to establishing a symbiotic host-microbe micro-environment. *Am. J. Pathol.* **178**, 1622–1634 (2011).
41. Kobayashi, K, Hernandez, L.D., Galan, J.E., Janeway, C.A. Jr, Medzhitov, R & Flavell, R.A. IRAK-M is a negative regulator of Toll-like receptor signaling. *Cell* **110**, 191–202 (2002).
42. Flannery, S & Bowie, A.G. The interleukin-1 receptor-associated kinases: critical regulators of innate immune signalling. *Biochem. Pharmacol.* **80**, 1981–1991 (2010).
43. Cole, T.S. *et al.* IRAK-M modulates expression of IL-10 and cell surface markers CD80 and MHC II after bacterial re-stimulation of tolerized dendritic cells. *Immunol. Lett.* **144**, 49–59 (2012).
44. Matsunaga, K, Klein, T.W., Friedman, H & Yamamoto, Y. Alveolar macrophage cell line MH-S is valuable as an in vitro model for Legionella pneumophila infection. *Am. J. Respir. Cell Mol. Biol.* **24**, 326–331 (2001).
45. Sendide, K, Deghmane, A.E., Pechkovsky, D, Av-Gay, Y, Talal, A & Hmama, Z. Mycobacterium bovis BCG attenuates surface expression of mature class II molecules through IL-10-dependent inhibition of cathepsin S. *J. Immunol.* **175**, 5324–5332 (2005).
46. Jacobs, M, Fick, L, Allie, N, Brown, N & Ryffel, B. Enhanced immune response in Mycobacterium bovis bacille calmette guerin (BCG)-infected IL-10-deficient mice. *Clin. Chem. Lab. Med.* **40**, 893–902 (2002).
47. Jeyanathan, M. *et al.* Airway delivery of soluble mycobacterial antigens restores protective mucosal immunity by single intramuscular plasmid DNA tuberculosis vaccination: role of proinflammatory signals in the lung. *J. Immunol.* **181**, 5618–5626 (2008).
48. Kohlmeier, J.E. *et al.* The chemokine receptor CCR5 plays a key role in the early memory CD8+ T cell response to respiratory virus infections. *Immunity* **29**, 101–113 (2008).
49. Beisiegel, M. *et al.* Combination of host susceptibility and virulence of Mycobacterium tuberculosis determines dual role of nitric oxide in the protection and control of inflammation. *J. Infect. Dis.* **199**, 1222–1232 (2009).
50. Myers, A.J., Marino, S, Kirschner, D.E. & Flynn, J.L. Inoculation dose of Mycobacterium tuberculosis does not influence priming of T cell responses in lymph nodes. *J. Immunol.* **190**, 4707–4716 (2013).
51. Torrelles, J.B. & Schlesinger, L.S. Diversity in Mycobacterium tuberculosis mannosylated cell wall determinants impacts adaptation to the host. *Tuberculosis (Edinb)* **90**, 84–93 (2010).
52. Pathak, S.K., Basu, S, Bhattacharyya, A, Pathak, S, Kundu, M & Basu, J. Mycobacterium tuberculosis lipoarabinomannan-mediated IRAK-M induction negatively regulates Toll-like receptor-dependent interleukin-12 p40 production in macrophages. *J. Biol. Chem.* **280**, 42794–42800 (2005).
53. Almeida, A.S. *et al.* Tuberculosis is associated with a down-modulatory lung immune response that impairs Th1-type immunity. *J. Immunol.* **183**, 718–731 (2009).
54. Bonecini-Almeida, M.G. *et al.* Down-modulation of lung immune responses by interleukin-10 and transforming growth factor beta (TGF-beta) and analysis of TGF-beta receptors I and II in active tuberculosis. *Infect. Immun.* **72**, 2628–2634 (2004).
55. Jamil, B. *et al.* Interferon gamma/IL10 ratio defines the disease severity in pulmonary and extra pulmonary tuberculosis. *Tuberculosis (Edinb)* **87**, 279–287 (2007).
56. Nochi, H. *et al.* Modulation of hepatic granulomatous responses by transgene expression of DAP12 or TREM-1-Ig molecules. *Am. J. Pathol.* **162**, 1191–1201 (2003).
57. Turnis, M.E. *et al.* IRAK-M removal counteracts dendritic cell vaccine deficits in migration and longevity. *J. Immunol.* **185**, 4223–4232 (2010).
58. Norton, J.T., Hayashi, T, Crain, B, Corr, M & Carson, D.A. Role of IL-1 receptor-associated kinase-M (IRAK-M) in priming of immune and inflammatory responses by nitrogen bisphosphonates. *Proc. Natl. Acad. Sci. USA* **108**, 11163–11168 (2011).
59. O'Garra, A, Barrat, F.J., Castro, A.G., Vicari, A & Hawrylowicz, C. Strategies for use of IL-10 or its antagonists in human disease. *Immunol. Rev.* **223**, 114–131 (2008).
60. Santosuosso, M. *et al.* Mucosal luminal manipulation of T cell geography switches on protective efficacy by otherwise ineffective parenteral genetic immunization. *J. Immunol.* **178**, 2387–2395 (2007).
61. Santosuosso, M, Zhang, X, McCormick, S, Wang, J, Hitt, M & Xing, Z. Mechanisms of mucosal and parenteral tuberculosis vaccinations: adenoviral-based mucosal immunization preferentially elicits sustained accumulation of immune protective CD4 and CD8 T cells within the airway lumen. *J. Immunol.* **174**, 7986–7994 (2005).
62. Kugathasan, K, Roediger, E.K., Small, C.L., McCormick, S, Yang, P & Xing, Z. CD11c+ antigen presenting cells from the alveolar space, lung parenchyma and spleen differ in their phenotype and capabilities to activate naive and antigen-primed T cells. *BMC Immunol.* **9**, 48 (2008).
63. Xing, Z, Ohkawara, Y, Jordana, M, Graham, F & Gauldie, J. Transfer of granulocyte-macrophage colony-stimulating factor gene to rat lung induces eosinophilia, monocytosis, and fibrotic reactions. *J. Clin. Invest.* **97**, 1102–1110 (1996).